Connecting EPBM Data to Ground Movement Data using Machine Learning

Dayu Apoji, S.M.ASCE[1], Zhangwei Ning, Ph.D., M.ASCE[2], and Kenichi Soga, Ph.D., F.ASCE[3]

[1]Department of Civil and Environmental Engineering, University of California Berkeley, Berkeley, CA 94720-1234; E-mail: dayu.apoji@berkeley.edu
[2]Sixense Inc., Bothell, WA 98011; E-mail: zhangwei.ning@sixense-group.com
[3]Department of Civil and Environmental Engineering, University of California Berkeley, Berkeley, CA 94720-1234; E-mail: soga@berkeley.edu

ABSTRACT

This paper presents a method to estimate tunneling-induced ground movements by connecting the earth pressure balance tunnel boring machine (EPBM) operation data to the ground monitoring data. The proposed method requires no prior assumptions, such as the ground loss and the geologic parameters. This study was conducted using a data set from the State Route 99 (SR99) tunnel project in Seattle, WA. The prediction models were developed using (i) ordinary least squares (OLS) as a parametric linear regression method and (ii) random forests (RF) as a nonparametric nonlinear machine learning method. Segmentation and feature importance analyses were carried out to investigate the influence of EPBM features on the induced ground movements in different ground-machine interaction mechanisms. This study shows that various tunneling-induced ground responses can be estimated solely based on the EPBM feature data and the tunnel spatial geometries. The segmentation and feature importance analyses reveal that each ground response segment has different governing parameters. Features related to the steering and pressure controls appear to influence the induced ground movements during the EPBM passing strongly. These features are not typically considered in conventional tunneling-induced ground movement prediction methods.

INTRODUCTION

Tunneling-induced ground movements are mainly governed by (i) the tunnel spatial geometries, (ii) the geologic conditions, and (iii) the tunneling processes, i.e., the tunnel boring machine (TBM) behaviors. Conventionally, the movements can be estimated using various methods, for instance, empirical (Mair and Taylor 1999; Peck 1969), analytical (Loganathan and Poulos 1998; Pinto and Whittle 2014), and numerical methods (Avgerinos et al. 2018; Kasper and Meschke 2004; Komiya et al. 1999). Each method offers different approaches, but the key inputs are always dominated by the tunnel spatial geometries and the geologic conditions. Limited attention has been given to the effects of TBM behaviors.

Studies have been conducted to incorporate more information related to TBM behaviors in tunneling-induced ground movement models. Most of the studies utilized TBM operation data and machine learning algorithms. In early development, Shi (1998) developed a tunneling-induced ground movement model using the artificial neural network (ANN) with TBM advance rates as one of the model input variables. Subsequently, more TBM features (operation variables) were included as input variables in the prediction models, e.g., Suwansawat and Einstein (2006) and Boubou et al. (2010) used 5 and 10 TBM features for their ANN models, respectively. More variation of machine learning algorithms has also been implemented, e.g., the Gaussian Process Regression (GPR), Support Vector Machine (SVM), Random Forests (RF), and deep neural networks. Several comparative studies show that RF often delivered the best and the most stable prediction performance (Chen et al. 2019; Ling et al. 2022; Tang and Na 2021; Zhang et al. 2020).

Despite these developments, most previous studies merely focused on predicting the cross-sectional maximum ground settlement. Less attention has been given to predicting the longitudinal ground responses during TBM passing and the effects of TBM control parameters. Furthermore, many studies still reported conflicting results on the feature importance analysis. This study aims to develop a method to estimate the longitudinal tunneling-induced ground movements by connecting the TBM operation data to the ground monitoring data. The proposed method estimates the longitudinal ground response during TBM passing solely based on the TBM features and the tunnel spatial geometries.

This study was conducted using an earth pressure balance TBM (EPBM) data set and a multipoint borehole extensometer (MPBX) data set from the State Route 99 (SR99) tunnel project in Seattle, WA. The models were developed using two prediction methods: (i) a parametric linear regression method and (ii) a nonparametric nonlinear machine learning method. Feature importance analysis was performed to investigate the influence of TBM features on the induced ground movements. Segmentation analysis was also performed to investigate different ground-machine interaction mechanisms.

DATA AND METHODS

Tunneling Case. The SR99 is a highway tunnel with a length of 2830 m (1.756 mi) and a maximum depth of 65.5 m (215 ft) below the ground surface. The tunnel was constructed using a double shield EPBM with a 17.5 m (57.5 ft) diameter. The geologic conditions along the tunnel alignment were dominated by over-consolidated glacial and non-glacial pre-Vashon geologic units. The surficial geologic conditions were dominated by recent granular deposits, clay, silt, and fills (WSDOT 2010a; b).

EPBM Data. The EPBM produced numerous sensor measurements every 5 seconds during the tunneling operation. In this study, the observation points were represented in spatial series as chainage locations per ring advance. Depending on the data characteristics, an observation point

can be the final observation value of one ring advance (e.g., features related to volume and length measurements) or the average value over one ring advance (e.g., features related to pressure, forces, speed measurements).

To allow better interpretability of the models, this study only considered continuous measurements data from the primary EPBM functional systems, i.e., features related to (i) excavation, (ii) advancing, (iii) steering, (iv) ground conditioning, (v) earth pressure balancing, (vi) muck extraction, and (vii) tail grouting. Records from the same sensor types and measurements were aggregated to further condense the number of features. The data was cleaned by removing the observations of non-advancing phases, erroneous records, missing values, and features with constant variables. This data preparation resulted in a total of 28 EPBM features and 1253 observation points.

Ground Movement Data. The tunneling-induced ground movements along the tunnel alignment were measured using various monitoring instruments (Ning et al. 2019). To limit the scope, this study only considered underground movement data from MPBX at 5 ft (approx. 1.5 meters, MPBX code 01) and 10 ft (approx. 3 meters, MPBX code 02) distances above the tunnel crown. This selection resulted in a total of 159 MPBX locations. Note that the measured underground movements are the relative movement of a particular point to the ground surface movement. To limit the data size, this preliminary study uses the daily median records.

Data Integration. The EPBM data frame consisted of the operation features at each chainage head position and the corresponding time record. The MPBX data frame consisted of the recorded ground movements of each monitoring point chainage position and the corresponding distance to the center of tunnel alignment, distance to the tunnel crown, and the time record. Both data frames were connected by the time record column. This means one row of EPBM data at a particular chainage head position can correspond to ground movement records from several MPBX locations. Subsequently, distances from the EPBM head to each MPBX location can be obtained. The connection between an MPBX location and the EPBM position at a time is illustrated in Figure 1.

Model Setup. The data-driven model was developed to estimate the ground response, y, at a particular location l, and at time t as a function of the tunnel spatial geometries (TSG) at time t, and the 28 EPBM features ($EPBM_{ops}$) at time t,

$$y_l(t) = f\left(TSG(t), EPBM_{ops}(t)\right).$$

The tunnel spatial geometries consisted of (i) distance to the EPBM head, (ii) distance to the center of tunnel alignment, (iii) distance to the tunnel crown, and (iv) the tunnel depth. Including the 28 EPBM features, this gave a total of 32 input features for the models.

Explicit information on the geologic conditions was not used since this information has been implicitly contained in the interactions among the EPBM features (Apoji et al. 2022; Sousa and Einstein 2012). In this study, the tunneling effects were considered negligible at -50 m

before and 100 m after EPBM passing. Observations on the longitudinal ground movements during EPBM passing have been reported by Wan et al. (2017a; b).

The merged data set was split randomly in a 70:30 ratio to divide the training and testing data sets. This random splitting scheme may not be feasible for actual tunneling where the data are generated in a sequence. However, this scheme was selected to provide a preliminary study with ideal randomized training data. The prediction results were evaluated using the mean absolute errors (MAE). The data-driven model pipeline is illustrated in Figure 2.

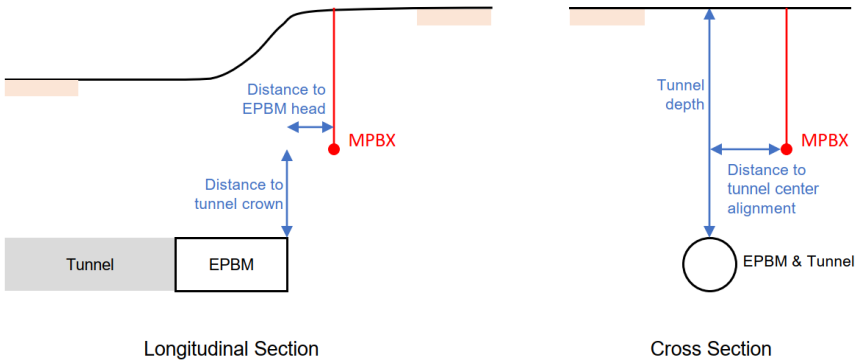

Figure 1. The connection between an MPBX location and the EPBM position at a time.

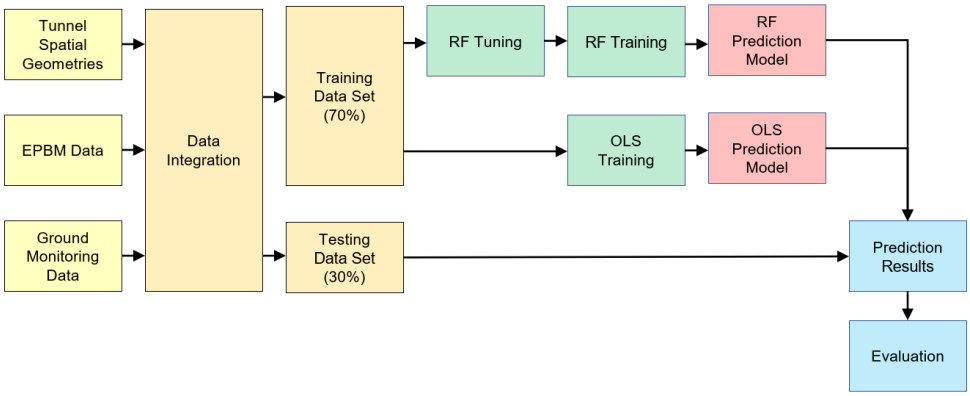

Figure 2. Data-driven model pipeline.

Prediction Methods. The ground movement model was developed using two data-driven prediction methods: (i) the ordinary least squares (OLS) and (ii) the random forests (RF). OLS was selected as a benchmark method to represent a parametric linear regression method. OLS constructs the model by minimizing the residual sum squares (RSS),

$$RSS = \sum_{i=1}^{n} \left(y_i - \left(\hat{\beta}_0 + \hat{\beta}_1 x_{i1} + \hat{\beta}_2 x_{i2} + \cdots + \hat{\beta}_p x_{ip} \right) \right)^2,$$

where i is an observation point, y is the response, x_1 to x_p are the predictors, and $\hat{\beta}_0$ to $\hat{\beta}_p$ are the estimated regression coefficients.

RF was selected to represent a nonparametric and nonlinear machine learning prediction method. RF is an ensemble supervised learning algorithm that produces its prediction by aggregating a large number of decision trees as the base learners (Breiman 2001). RF was selected since this method has straightforward hyperparameter tuning and performs excellently in tabular data (Grinsztajn et al. 2022). The method is also robust to noises and less prone to overfit (Liu et al. 2012). Furthermore, as a nonparametric method, RF does not require the data to meet certain assumptions or parameters (Malley et al. 2012). Briefly, RF algorithm is performed by

(i) generating B bootstrapped training data sets;

(ii) constructing decision trees, $\hat{f}^{*b}(x)$, using each of the b^{th} bootstrapped data sets;

(iii) aggregating all the constructed decision tree results to obtain the final result,

$$\hat{f}_{bag}(x) = \frac{1}{B}\sum_{b=1}^{B} \hat{f}^{*b}(x).$$

A single decision tree is constructed using binary recursive partitioning into distinct subsets so that one parent node leaves two child nodes (Therneau and Atkinson 1997). The selected predictors, x_j, and the cutpoint, s, can be determined by minimizing the residual sum of squares (RSS),

$$RSS = \sum_{i:x_i \epsilon R_1(j,s)} \left(y_i - \hat{y}_{R_1}\right)^2 + \sum_{i:x_i \epsilon R_2(j,s)} \left(y_i - \hat{y}_{R_2}\right)^2.$$

where $\hat{y}$ is the estimated responses of the pair of half-planes R_1 and R_2 (James et al. 2013). This study was performed in R programming language using the fast implementation of RF in C++ (Wright and Ziegler 2017).

Hyperparameter Tuning. Hyperparameter evaluation was performed on the training data set to investigate the effects of RF hyperparameters on the prediction performance and to select the best hyperparameters for the analysis. The evaluation was performed in 5-times repeated 10-folds cross-validation (CV) analysis, using various ranges of RF hyperparameters, i.e., (i) the possible number of features that are randomly selected to split at each branch node (mtry), (ii) the minimum node size of the end leaf, and (iii) the number of grown trees (ntrees). The validation performance was evaluated using the out-of-bag (OOB) data sets.

Feature Importance Analysis. The permutation-based feature importance analysis was employed to obtain RF feature importance scores. Briefly, the permutation feature importance measures the difference in prediction errors between the original data set and the data set with a particular feature being permuted (Gregorutti et al. 2017; Nicodemus et al. 2010). Higher scores mean higher prediction errors when a particular feature is permuted, indicating its importance in the prediction model. The permutation-based importance was selected since it is less susceptible to bias than the standard RF impurity-based importance (Altmann et al. 2010; Strobl et al. 2007).

Segmentation Analysis. Segmentation analysis was performed to investigate different ground response mechanisms relative to EPBM positions. The analysis was performed by segmenting RF model with a moving boundary line throughout the ground responses. A segment was defined as a distance where the model produced negligible prediction errors. However, a threshold MAE of 0 mm produces a very sensitive analysis, i.e., too many segments. Therefore, this study used a threshold MAE of 0.2 mm to allow better interpretability. The next segment was created similarly by starting the new moving boundary from the end boundary of the previous segment. The algorithm of the segmentation analysis is presented in Table 1.

Table 1. Segmentation analysis

No.	Algorithm
	Input: training and testing data sets from randomly splitted instrument IDs
	Output: SegmentBoundary, SegmentMAE
1	**Initialize**
	StartBoundary = -50 m
	EndBoundary = 100 m
	ErrorThreshold = 0.2 mm
3	**While** (StartBoundary < EndBoundary)
4	**Initialize** SegmentMAE
5	**For** (b in StartBoundary to EndBoundary)
6	Slice data from StartBoundary to b
7	Get training and testing data sets within the slice
8	Train model
9	**Initialize** InstrumentMAE
10	**For** (each instrument in the testing data set)
11	Get prediction
12	Get and store InstrumentMAE
13	Get and store SegmentMAE as InstrumentMAE at boundary b
14	Get and store SegmentBoundary as the last b where MAE < ErrorThreshold
15	Update StartBoundary as SegmentBoundary at the current iteration

RESULTS AND DISCUSSION

Effects of Hyperparameters. Figure 3 presents the effects of RF hyperparameters on the OOB predictions. The left panel presents the effect of the ntrees parameter on the MAE in various mtry parameters, with a constant minimum node size parameter of 1. The figure shows that a low number of ntrees (e.g., ntrees < 200) produced lower prediction performance. Increasing the ntrees improved the prediction performance significantly until it reached the threshold value and stabilized. This result agrees with previous studies, either using the EPBM data set (Apoji et al. 2022) or other data sets (Probst et al. 2019). In this study, ntrees of 500 were selected for the model to ensure high prediction performance and reasonable computation costs.

The right panel presents the effect of the mtry parameter on the MAE in various minimum node size parameters, with a constant ntrees parameter of 500. This figure shows that higher numbers of mtry produced lower MAE, which means higher prediction performance. The best prediction performance was produced when the mtry was equal to the number of predictors (i.e., p = 32). This is an interesting finding since the best prediction performance for an RF regression is typically produced by mtry = p/3 (e.g., Apoji et al. 2022; Probst et al. 2019). The minimum node sizes produced fewer effects on the prediction performance. The best prediction performance was produced at the minimum node sizes of 1 and 3. The large mtry and small minimum node size values indicate that more complex trees were required for the predictions. This hyperparameter configuration reveals the complexity of the relationship between EPBM and the ground responses. In this study, mtry of p = 32 and the minimum node size of 1 were selected for the models.

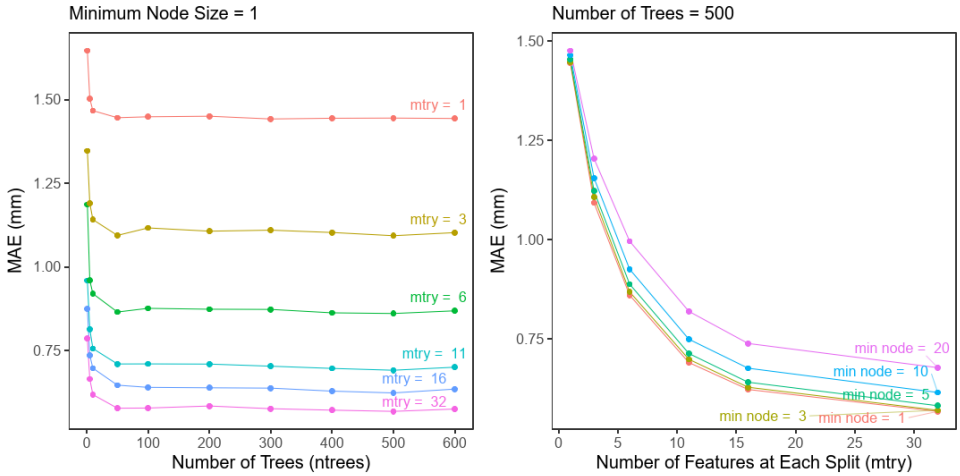

Figure 3. Effects of RF hyperparameters on the OOB predictions (training data set).

Ground Movement Predictions. Figure 4 presents several selected tunneling-induced ground movement predictions from the testing data set. The x-axes show the distance from the measurement points (MPBX locations) to the EPBM head (in meters). The y-axes show the induced ground movements (in mm). The measured ground responses are shown in black. The OLS and RF predictions are shown in red and blue, respectively. The figure presents different types of induced ground responses, i.e., settlement (panels in the left column), heaving (the middle column), and relatively stable responses (the right column). The selected responses show the variability of tunneling-induced ground movements. Note that the simplified model, such as the Gaussian settlement profile-based models, may not be able to capture this variability.

These figures show that the RF model could predict tunneling-induced ground movements solely based on the EPBM data. The predicted ground responses are in reasonably good agreement with the measured responses. In contrast, the OLS model could not reconstruct the measured responses, with substantial discrepancies in both pattern and magnitude of the ground movements. This result indicates the presence of nonlinear interactions between the EPBM and the ground responses. This nonlinearity could not be captured by OLS, which is a

parametric model that strictly constrains the fitting to be linear. This result suggests the value of nonparametric machine learning methods to model data sets with complex interactions.

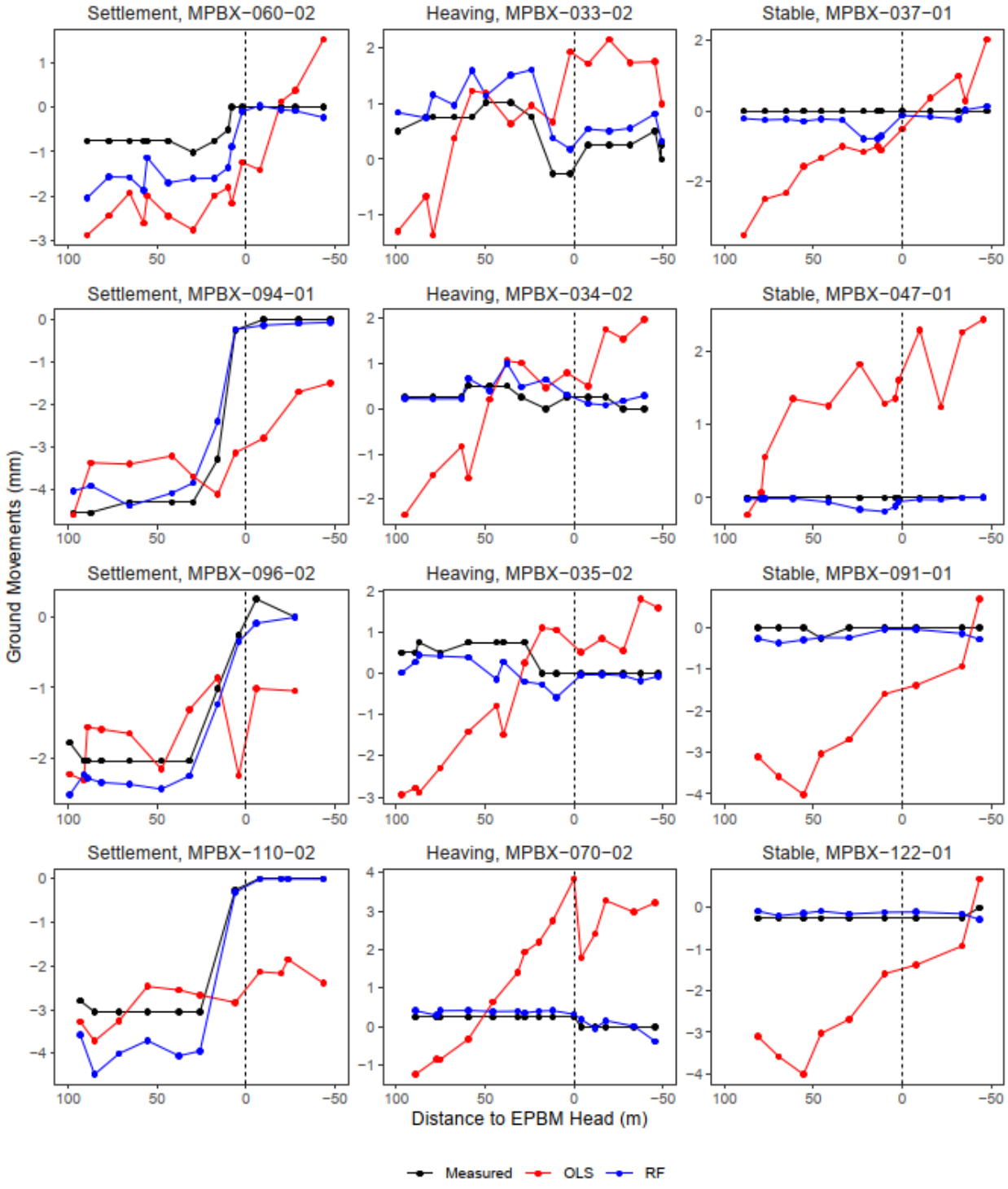

Figure 4. Selected tunneling-induced ground movement predictions with different types of responses from the testing data set: settlement (panels in the left column), heaving (the middle column), and relatively stable responses (the right column).

Figure 5 presents the absolute error (y-axis, in mm) of every monitoring point relative to the EPBM head distance (x-axis, in meters) from all predictions in the testing data set. The absolute errors of the OLS and RF models are shown in red and blue, respectively. The Locally Estimated Scatterplot Smoothing (LOESS) lines are shown to represent the scattering data points visually. Note that LOESS is essentially a generalization form of moving average and polynomial regression (Garimella 2017). The figure shows that the overall RF model performance was better than the overall OLS model. The RF models produced relatively small errors at points ahead of the EPBM (before passing).

In contrast, the OLS model produced substantial errors in this segment. It even failed to capture zero ground movements at 50-meter distances ahead of the EPBM. Note that all the training data were set to zero at this point. Both models exhibited increases in errors during EPBM passing. Subsequently, the errors stabilized after the passing. This indicates different mechanisms of EPBM and ground interactions before, during, and after EPBM passing.

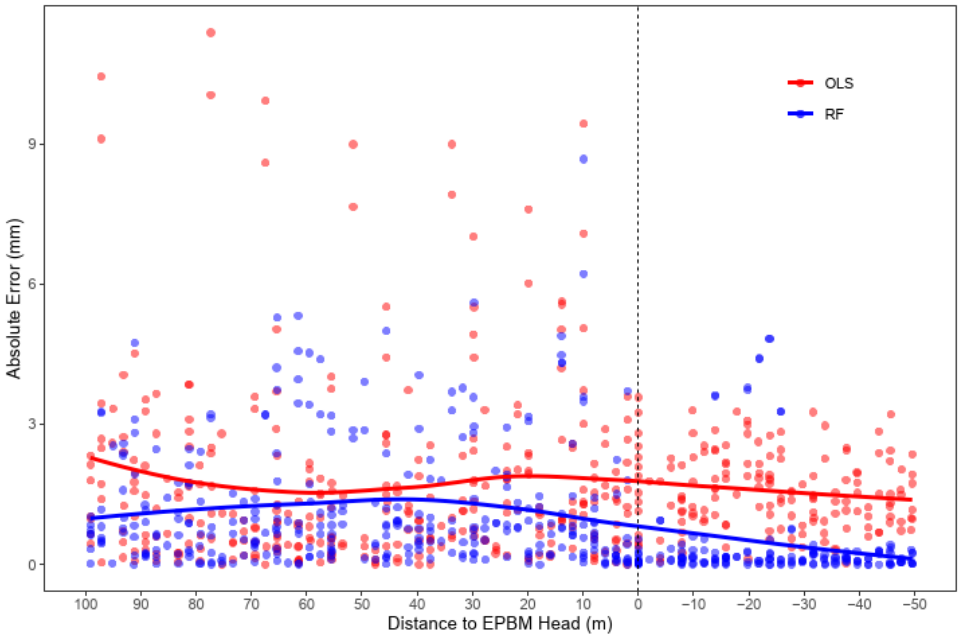

Figure 5. Absolute error of every monitoring point relative to the EPBM head distance from all predictions in the testing data set.

Ground Response Segmentation. Figure 6 presents ground response segments based on the segmentation analysis. Each segment is shown as a distance between two dashed boundary lines (red), where the model produces negligible errors (MAE < 0.2 mm). In this case, the first segment is produced from -50 to 3 m to the EPBM head. This segment may represent the ground response ahead of the EPBM. The second, third, and fourth segments are produced from 3 to 7 m, 7 to 13 m, and 13 to 21 m to the EPBM head, respectively. These segments may represent the ground response during the EPBM passing. The fifth segment is produced from 21 to 31 m, representing the post-tunneling ground response over the newly constructed tunnel lining. The

sixth and seventh segments are from 31 to 95 m and 95 to 100 m to the EPBM head, respectively. These segments may represent post-tunneling ground responses in the longer term. The smaller segment size during EPBM passing may indicate a more complex ground response mechanism during this period.

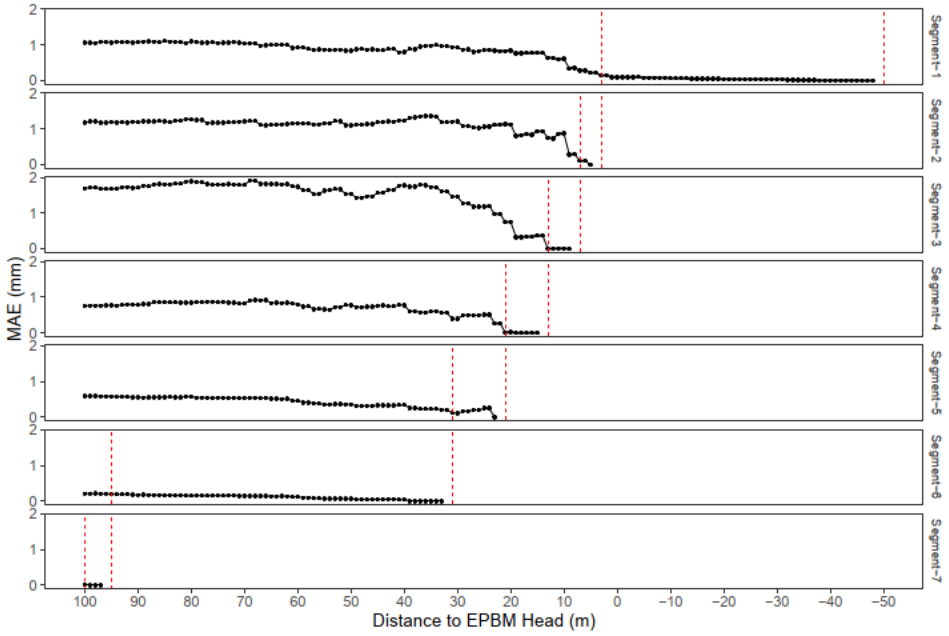

Figure 6. Ground response segments based on the segmentation analysis. Each segment produces MAE < 0.2 mm and is shown as a distance between the two red dashed boundary lines.

Feature Importance for Overall Response. Figure 7 presents the feature importance rank of the overall ground response RF model (a segment from -50 m to 100 meters distance to the EPBM head). The rank shows that spatial geometries (i.e., the distance from the point of interest to the center of tunnel alignment, the tunnel depth, as well as the distance from the point of interest to the EPBM head and crown) were the key parameters in estimating the ground responses. The conventional tunneling-induced ground movement prediction methods have also considered the geometrical information in the models.

Interestingly, features related to steering control (i.e., pitch, yaw, and deviation) and chamber pressure were in high-importance ranks. Note that these features are not commonly included as specific parameters in conventional prediction methods. This suggests that TBM control parameters substantially govern the induced ground movement and should be considered more carefully in tunneling-induced prediction models.

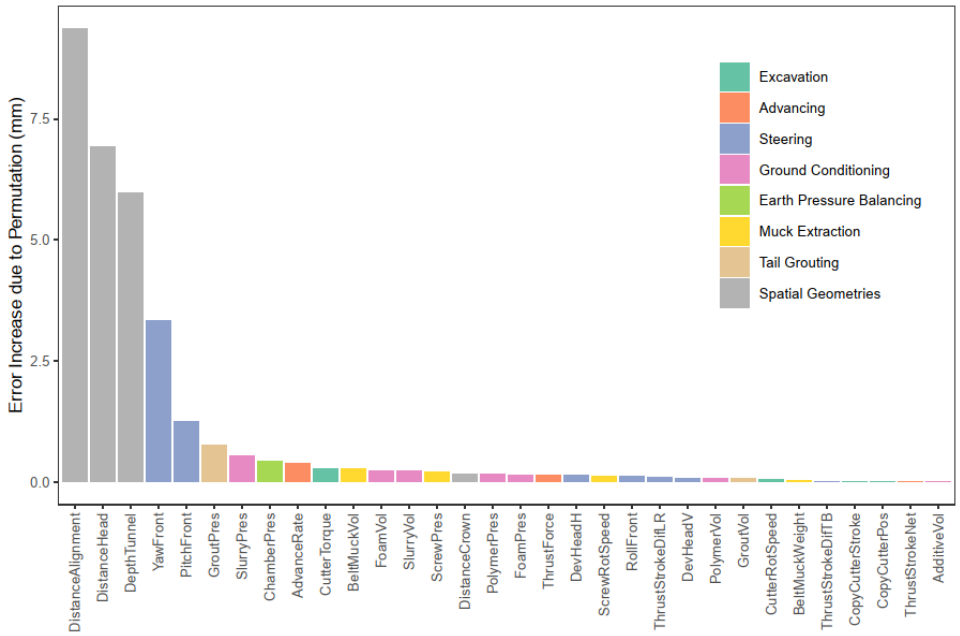

Figure 7. RF feature importance rank of the overall ground response model

Feature Importance for Segmental Responses. Figure 8 presents simplified ground response segments (top panel) and feature importance ranks of each segment (bottom panels). The simplified ground response segments were approximated based on the segmentation analysis result. The feature importance ranks only show the top 8 features, to focus on the most critical features in the predictions. The figure shows that each ground response segment produced different feature ranks, indicating different TBM-ground interaction mechanisms. The simplified ground response segments are described below.

- Segment 1 represents the ground response ahead of the EPBM. This segment appears to be dominated by geometrical parameters. This suggests that the ground response mainly depends on the distance to the EPBM.
- Segment 2 represents the ground response over the EPBM front shield. This segment indicates a strong influence of the screw-related features. Note that these features can be related to how the operators control the chamber pressure. This suggests the critical role of pressure control on the ground response.
- Segment 3 represents the ground response over the EPBM articulation and rear shield. This segment shows domination from features related to the steering control (i.e., deviation and thrust stroke difference).
- Segment 4 represents the post-tunneling ground response over the newly constructed tunnel lining. This segment appears to be dominated by the geometrical parameters and the muck volume (which may be related to the ground loss).
- Segment 5 represents the longer-term post-tunneling ground behavior. This segment is strongly dominated by features related to the ground conditioning system, i.e., the polymer volume. Note that polymer volume is typically injected to minimize the

stickiness of clayey soils (Todaro et al. 2021). This indicates that the ground response mainly depends on the soil type, e.g., more long-term settlement is expected on clayey soils.

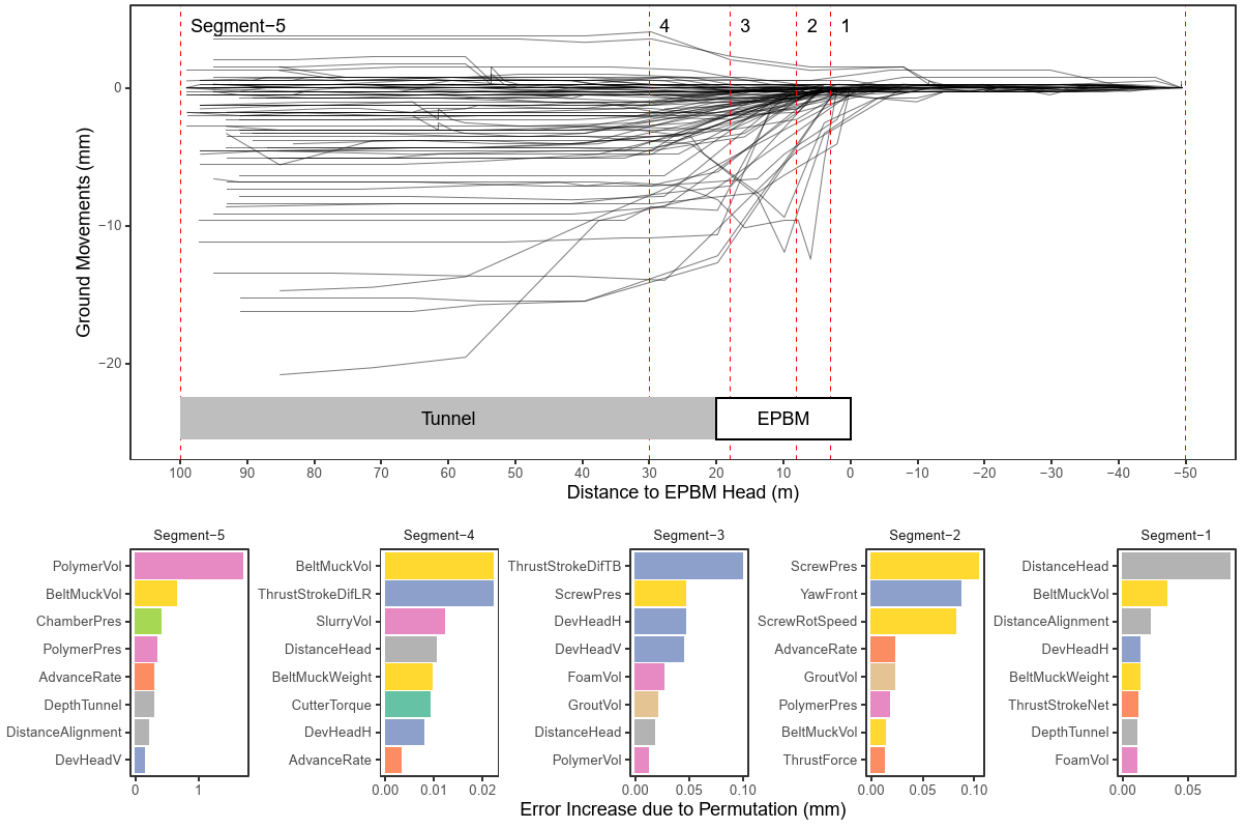

Figure 8. RF feature importance rank of each ground response segment.

CONCLUSIONS

The feasibility of a data-driven method that connects EPBM data to the ground monitoring data has been demonstrated. The developed model can predict various types of tunneling-induced ground movements solely based on the EPBM features and the tunnel spatial geometries without any prior assumption on the ground loss and the geologic parameters. The nonparametric and nonlinear machine learning prediction model produces better estimations than the parametric linear regression model. This indicates the complexity and nonlinearity of TBM-ground interactions.

The segmentation analysis shows tunneling-induced ground movements can be divided into several ground response segments relative to the EPBM positions, indicating different TBM-ground interaction mechanisms at each ground response segment. Furthermore, the feature importance analysis reveals that each segment may have different controlling parameters. Features related to the steering and pressure controls appear to influence the induced ground

movements during EPBM passing strongly. These features are not typically considered in conventional tunneling-induced ground movement estimation methods.

A development of this method may include incorporating records from multi-instruments with a finer resolution of both TBM and ground monitoring data. A more robust feature importance analysis and the effects of the threshold value should also be examined. The dynamic sequential prediction model should be developed to enable the implementation of this data-driven method in actual tunnel construction.

ACKNOWLEDGEMENTS

The first author acknowledged scholarship and research support from the Indonesia Endowment Fund for Education (LPDP) and the Department of Civil and Environmental Engineering, University of California at Berkeley. The authors thank Yuji Fujita (Enzan Koubou, Co. Ltd.) for valuable discussions during this research. The data used in this study was obtained from the Washington State Department of Transportation (WSDOT) and Sixense, Inc., with permission from WSDOT.

REFERENCES

Altmann, A., L. Toloşi, O. Sander, and T. Lengauer. 2010. "Permutation importance: a corrected feature importance measure." *Bioinformatics*, 26 (10): 1340–1347. https://doi.org/10.1093/bioinformatics/btq134.

Apoji, D., Y. Fujita, and K. Soga. 2022. "Soil Classification and Feature Importance of EPBM Data Using Random Forests." 520–528. American Society of Civil Engineers. https://doi.org/10.1061/9780784484029.052.

Avgerinos, V., D. M. Potts, J. R. Standing, and M. S. P. Wan. 2018. "Predicting tunnelling-induced ground movements and interpreting field measurements using numerical analysis: Crossrail case study at Hyde Park." *Géotechnique*, 68 (1): 31–49. https://doi.org/10.1680/jgeot.16.P.219.

Boubou, R., F. Emeriault, and R. Kastner. 2010. "Artificial neural network application for the prediction of ground surface movements induced by shield tunnelling." *Can. Geotech. J.*, 47 (11): 1214–1233. NRC Research Press. https://doi.org/10.1139/T10-023.

Chen, R., P. Zhang, H. Wu, Z. Wang, and Z. Zhong. 2019. "Prediction of shield tunneling-induced ground settlement using machine learning techniques." *Front. Struct. Civ. Eng.*, 13 (6): 1363–1378. https://doi.org/10.1007/s11709-019-0561-3.

Garimella, R. V. 2017. *A Simple Introduction to Moving Least Squares and Local Regression Estimation*. LA--UR-17-24975, 1367799.

Gregorutti, B., B. Michel, and P. Saint-Pierre. 2017. "Correlation and variable importance in random forests." *Stat Comput*, 27 (3): 659–678. https://doi.org/10.1007/s11222-016-9646-1.

Grinsztajn, L., E. Oyallon, and G. Varoquaux. 2022. "Why do tree-based models still outperform deep learning on tabular data?" arXiv.

James, G., D. Witten, T. Hastie, and R. Tibshirani. 2013. *An Introduction to Statistical Learning: with Applications in R*. Springer Science & Business Media.

Kasper, T., and G. Meschke. 2004. “A 3D finite element simulation model for TBM tunnelling in soft ground.” *International Journal for Numerical and Analytical Methods in Geomechanics*, 28 (14): 1441–1460. https://doi.org/10.1002/nag.395.

Komiya, K., K. Soga, H. Akagi, T. Hagiwara, and M. D. Bolton. 1999. “Finite Element Modelling of Excavation and Advancement Processes of a Shield Tunnelling Machine.” *Soils and Foundations*, 39 (3): 37–52. https://doi.org/10.3208/sandf.39.3_37.

Ling, X., X. Kong, L. Tang, Y. Zhao, W. Tang, and Y. Zhang. 2022. “Predicting earth pressure balance (EPB) shield tunneling-induced ground settlement in compound strata using random forest.” *Transportation Geotechnics*, 35: 100771. https://doi.org/10.1016/j.trgeo.2022.100771.

Liu, Y., Y. Wang, and J. Zhang. 2012. “New Machine Learning Algorithm: Random Forest.” *Information Computing and Applications*, Lecture Notes in Computer Science, B. Liu, M. Ma, and J. Chang, eds., 246–252. Berlin, Heidelberg: Springer.

Loganathan, N., and H. G. Poulos. 1998. “Analytical Prediction for Tunneling-Induced Ground Movements in Clays.” *Journal of Geotechnical and Geoenvironmental Engineering*, 124 (9): 846–856. https://doi.org/10.1061/(ASCE)1090-0241(1998)124:9(846).

Mair, R. J., and R. N. Taylor. 1999. “Bored tunnelling in the urban environments.” *Fourteenth International Conference on Soil Mechanics and Foundation Engineering. ProceedingsInternational Society for Soil Mechanics and Foundation Engineering*.

Nicodemus, K. K., J. D. Malley, C. Strobl, and A. Ziegler. 2010. “The behaviour of random forest permutation-based variable importance measures under predictor correlation.” *BMC Bioinformatics*, 11 (1): 110. https://doi.org/10.1186/1471-2105-11-110.

Ning, Z., L. Galisson, and P. Smith. 2019. “Case Study: Geotechnical Instrumentation and Monitoring of Alaskan Way Viaduct Replacement Project.” 10. ASCE.

Peck, R. B. 1969. “Deep Excavation and Tunneling in Soft Ground. State-of-the-Art Report.” *Proceedings of the 7th International Conference on Soil Mechanics and Foundation Engineering, Mexico, 225-325.*

Pinto, F., and A. J. Whittle. 2014. “Ground Movements due to Shallow Tunnels in Soft Ground. I: Analytical Solutions.” *Journal of Geotechnical and Geoenvironmental Engineering*, 140 (4): 04013040. American Society of Civil Engineers. https://doi.org/10.1061/(ASCE)GT.1943-5606.0000948.

Probst, P., M. N. Wright, and A.-L. Boulesteix. 2019. “Hyperparameters and tuning strategies for random forest.” *WIREs Data Mining and Knowledge Discovery*, 9 (3): e1301. https://doi.org/10.1002/widm.1301.

Shi, J., J. a. R. Ortigao, and J. Bai. 1998. “Modular Neural Networks for Predicting Settlements during Tunneling.” *Journal of Geotechnical and Geoenvironmental Engineering*, 124 (5): 389–395. American Society of Civil Engineers. https://doi.org/10.1061/(ASCE)1090-0241(1998)124:5(389).

Sousa, R. L., and H. H. Einstein. 2012. “Risk analysis during tunnel construction using Bayesian Networks: Porto Metro case study.” *Tunnelling and Underground Space Technology*, 27 (1): 86–100. https://doi.org/10.1016/j.tust.2011.07.003.

Strobl, C., A.-L. Boulesteix, A. Zeileis, and T. Hothorn. 2007. “Bias in random forest variable importance measures: Illustrations, sources and a solution.” *BMC Bioinformatics*, 8 (1): 25. https://doi.org/10.1186/1471-2105-8-25.

Suwansawat, S., and H. H. Einstein. 2006. “Artificial neural networks for predicting the maximum surface settlement caused by EPB shield tunneling.” *Tunnelling and*

Underground Space Technology, 21 (2): 133–150. https://doi.org/10.1016/j.tust.2005.06.007.
Tang, L., and S. Na. 2021. "Comparison of machine learning methods for ground settlement prediction with different tunneling datasets." *Journal of Rock Mechanics and Geotechnical Engineering*, 13 (6): 1274–1289. https://doi.org/10.1016/j.jrmge.2021.08.006.
Todaro, C., A. Carigi, L. Peila, D. Martinelli, and D. Peila. 2021. "Soil conditioning tests of clay for EPB tunnelling." *Underground Space*. https://doi.org/10.1016/j.undsp.2021.11.002.
Wan, M. S. P., J. R. Standing, D. M. Potts, and J. B. Burland. 2017a. "Measured short-term ground surface response to EPBM tunnelling in London Clay." *Géotechnique*, 67 (5): 420–445. https://doi.org/10.1680/jgeot.16.P.099.
Wan, M. S. P., J. R. Standing, D. M. Potts, and J. B. Burland. 2017b. "Measured short-term subsurface ground displacements from EPBM tunnelling in London Clay." *Géotechnique*, 67 (9): 748–779. ICE Publishing. https://doi.org/10.1680/jgeot.SIP17.P.148.
Wright, M. N., and A. Ziegler. 2017. "ranger: A Fast Implementation of Random Forests for High Dimensional Data in C++ and R." *J. Stat. Soft.*, 77 (1). https://doi.org/10.18637/jss.v077.i01.
WSDOT. 2010a. *Interim Report CT-6: Geologic Characterization*. SR 99 Bored Tunnel Alternative Design-Build Project. Prepared by Shannon & Wilson, Inc.
WSDOT. 2010b. *Revised Geotechnical Baseline Report*. SR 99 Bored Tunnel Alternative Design-Build Project. Prepared by Parsons Brinckerhoff, Shannon & Wilson, Inc.
Zhang, P., H.-N. Wu, R.-P. Chen, T. Dai, F.-Y. Meng, and H.-B. Wang. 2020. "A critical evaluation of machine learning and deep learning in shield-ground interaction prediction." *Tunnelling and Underground Space Technology*, 106: 103593. https://doi.org/10.1016/j.tust.2020.103593.